Tropospheric precursors and stratospheric warmings

Judah Cohen

and

Justin Jones

Atmospheric and Environmental Research, Inc., Lexington, Massachusetts 02421, USA

Submitted to the Journal of Climate
October 22, 2010

Revised
February 3, 2011

2nd revision
April 13, 2011

3rd revision
June 2, 2011

Corresponding author address:
Judah Cohen
AER, Inc.,
131 Hartwell Avenue
Lexington, MA 02421
jcohen@aer.com

Abstract

Many tropospheric Arctic Oscillation (AO) events are preceded by stratospheric AO events and even earlier in time by anomalous upward energy flux associated with Rossby waves in the troposphere. Here we identify lower tropospheric circulation anomalies that precede large AO events in both the troposphere and the stratosphere and the anomalous upward energy flux. Compositing analysis of stratospheric warming events identifies regional tropospheric precursors, which precede stratospheric warmings. The tropospheric precursor is found to vary when compositing over polar vortex displacements and splits separately. Prior to vortex displacements the main anomaly sea level pressure center of the tropospheric precursor is located across northwest Eurasia and is associated with the Siberian high. Prior to vortex splits a similar anomaly center is identified in the tropospheric precursor but it is weaker and appears to be more strongly related to a shift in the storm tracks. Differences in the sea level pressure anomalies in the North Atlantic and the North Pacific are also observed when comparing the precursors prior to vortex displacements and splits. Identification of a unique tropospheric precursor to stratospheric warming and subsequently tropospheric AO events can help to improve our understanding of troposphere-stratosphere coupling. Furthermore, the observational evidence presented here can be compared with model simulations of winter climate variability and lead to potential model improvements.

1. Introduction

Prediction of the phase and magnitude of the dominant mode of Northern Hemisphere climate variability, referred to as the Arctic Oscillation (AO) or Northern Annular Mode (NAM), is considered the next most important anticipated advance in seasonal winter climate prediction (Cohen 2003). Studies have shown that on synoptic time scales, the variability in the phase of AO is due to wave breaking, e.g. Feldstein and Franzke (2006). Nonetheless, most studies on longer than synoptic time scales have emphasized the lack of understanding of the underlying dynamics driving AO variability and consequently its poor predictability (Seager et al. 2010).

It has been known for a relatively long time that planetary scale waves that propagate from the troposphere into the stratosphere control the zonal-mean stratospheric circulation and its variability (Charney and Drazin 1961; Matsuno 1970). Furthermore, later studies showed that it is variability within the troposphere that forces the changes in planetary waves that drives stratospheric variability (e.g., Ting and Held 1990; Scinocca and Haynes 1998). More recent work in turn argues that the zonal-mean stratospheric circulation can also exert a downward influence on the zonal-mean tropospheric circulation (Baldwin and Dunkerton 1999, 2001). Still, less is known about the time and meridional variation of the flow in the extratropical troposphere that triggers variability in the planetary waves, which then force stratospheric variability and eventually tropospheric variability on a hemispheric scale.

Eurasian snow cover has been shown to be a leading indicator of winter climate variability in both the troposphere and the stratosphere (Cohen and Entekhabi 1999; Cohen et al. 2007; Orsolini and Kvmatso 2009; Allen and Zender 2010; Smith et al. 2010). It has been postulated that snow cover influences hemispheric climate by forcing sea level pressure (SLP) and surface temperature anomalies across Northern Eurasia that in turn modulate the

large-scale vertically propagating energy fluxes that force stratospheric variability. A six-step conceptual model has been proposed on how regional perturbations or tropospheric precursors force first hemispheric-wide stratospheric variability followed by hemispheric-wide tropospheric variability (Cohen et al. 2007). There is an initial upward propagation of circulation and energy anomalies and a lagging downward propagation. The downward propagation has been well established at least statistically (Baldwin and Dunkerton 2001, 2003) if not physically (Plumb and Semeniuk 2003), however, variability in the lower troposphere that forces upward propagation of wave activity is less well understood (Cohen et al. 2007).

Anomalously extensive snow cover favors a strengthened Siberian high that acts as a tropospheric precursor to stratospheric warming and negative surface AO events (Cohen et al. 2001, 2002). Other observational and modeling studies have confirmed that tropospheric precursors to stratospheric warmings can be associated with Eurasian snow cover variability, El Niño/Southern Oscillation (ENSO) and atmospheric blocking. Martius et al. 2009 showed that atmospheric blocking up to ten days prior to the warming event precedes stratospheric warming events. Blocking in the Atlantic basin most often precedes vortex displacements while blocking in the Pacific basin often precedes vortex splits. Garfinkel et al. (2010) argue that both ENSO and Eurasian snow cover influence tropospheric height anomalies that force stratospheric variability. Kolstad and Charlton-Perez (2010) showed that climate models simulate tropospheric precursors, which precede stratospheric warming events similar to what is observed in the NCEP/NCAR reanalysis.

Stratospheric variability has been suggested as a long-lead predictor of winter weather (Baldwin et al. 2003). However, using stratospheric variability as a predictor in climate forecasts shows only marginal skill (e.g., Charlton et al. 2003) for three important reasons:

1. the duration and seasonality that the stratosphere and troposphere are coupled is short, 2. variability in the troposphere is more often than not independent of variability in the stratosphere and 3. the lead-time is shorter than is required for seasonal predictions. Identifying tropospheric precursors has the potential benefit of extending the lead-time of weather forecasts by predicting the phase of large tropospheric AO events weeks and even months in advance. However until now, long lead tropospheric precursors have not been clearly identified.

2. Data and Methods

For all atmospheric data we used the National Center for Environmental Prediction/National Center for Atmospheric Research (NCEP/NCAR) Reanalysis (Kalnay et al. 1996) 1948-2010. We repeated the analysis with the European Centre for Medium-Range Weather Forecasts (ECMWF) ERA-40 and Interim reanalyses (Uppala et al. 2006) and the results were not sensitive to the reanalysis chosen.

We defined a stratospheric warming as the reversal of the zonal-mean zonal wind from westerly to easterly at 60°N and 10 hPa to identify major stratospheric warming events (Manney et al. 2005; Charlton and Polvani 2007). The central date (day 0) of each stratospheric warming is defined as the first day that at 60°N and 10 hPa an easterly zonal-mean zonal wind is observed. All of our cases for vortex displacements and vortex splits (see Table 1) match this criteria in the NCEP/NCAR Reanalysis except for the 16 December 2000 event, however, this event featured an equatorward displacement of the polar vortex, record warm polar stratospheric temperatures, and record low December AO values.

For deriving the polar cap height anomalies we computed an area-weighted average of height anomalies poleward of 60°N at all available levels from 1000 hPa to 10 hPa (Cohen

et al. 2002). For the wave activity flux (WAF) we used the three-dimensional expansion of the two-dimensional Eliassen Palm flux derived by Plumb (1985). Previous studies showed that stratospheric warming events are preceded by anomalously strong upward WAF originating from the troposphere (e.g., Polvani and Waugh 2004; Cohen et al. 2007). Statistical significance was computed using a two-tailed Student's t-test and in our composite analysis we removed the daily mean before averaging by day and event.

3. Results

a. Precursors

In Figure 1, we composited SLP 45 days prior to and 45 days following a stratospheric warming event. Stratospheric warming events can occur in two different ways, vortex displacement and splits. During vortex displacements the polar vortex is shifted off the pole and during vortex splits the polar vortex is split into two pieces of comparable size. We then separated the stratospheric warming events into vortex displacement and vortex splitting events. In defining vortex displacements and vortex splits we followed the method of Charlton and Polvani (2007). Previous studies have shown that snow cover anomalies and SLP anomalies associated with the Siberian high prior to stratospheric warmings and winter AO events have more of a wave-one characteristic (Cohen et al. 2001, 2002), which are more closely associated with vortex displacements (Martius et al. 2009).

Following stratospheric warmings, the SLP fields are qualitatively similar, whether it is after vortex displacements or vortex splits with SLP anomalies showing positive values over the Arctic and negative values over the ocean basins (Panels 1b and 1d). This result is consistent with the analysis of Charlton and Polvani (2007). However, the 45-day period preceding the stratospheric warming event has similarities, but also some differences with

149 respect to SLP anomalies. For vortex displacements (Panel 1a), the Siberian high is
150 significantly strengthened to the northwest of the climatological center; this is the dominant
151 anomaly center in the Northern Hemisphere polar cap (see Figure 4 where prior to vortex
152 displacements a positive height anomaly is observed in the lower troposphere) and has been
153 argued to be associated with increased snow cover (Cohen et al. 2001; Garfinkel et al.
154 2010). There is also present an opposite low pressure anomaly associated with a deeper
155 Aleutian low, which has been argued to be associated with El Niño (Ineson and Scaife 2009;
156 Garfinkel et al. 2010). Together these two anomaly centers form a wave-one anomaly
157 pattern. Prior to vortex splits (Panel 1c), both of these features are present, but are weaker
158 and instead the most statistically significant feature is anomalous high pressure stretched
159 across the mid-latitudes of the North Pacific. The anomaly features resemble a wave train
160 emanating from the North Pacific and propagating over the Pole or an asymmetric shift in
161 the main storm tracks, with a northward shift in the North Pacific and a southward shift in
162 the North Atlantic. Together these anomaly centers more closely resemble a wave-two
163 anomaly pattern. This is consistent with the results of Martius et al. (2009) that showed that
164 a wave one pattern dominated the tropospheric height field prior to vortex displacements
165 and a wave two pattern dominated the tropospheric height field prior to vortex splits.

166 We analyzed all of the individual cases in our composites for vortex displacements and
167 splits and a positive SLP anomaly is found consistently in the northwest sector of Eurasia
168 among the individual cases, however, the location does vary from case to case and this
169 contributed to some damping of the anomaly. The primary tropospheric precursor to either
170 vortex displacements or splits is a center of anomalously high SLP primarily to the north or
171 northwest of the climatological position of the Siberian high. The positive SLP anomaly
172 associated with the Siberian high tends to be coupled in time with anomalously low SLP
173 over the Gulf of Alaska. The precursor SLP signal appears in almost every displacement

174 case sometime between 15 and 45 days prior to the warming. Although still common, a
175 general area of above normal SLP in northern Eurasia was observed less frequently in
176 vortex splits. Also, there are a number of instances in which positive SLP anomalies are
177 observed similar to those associated with major stratospheric warmings, but are followed by
178 either minor stratospheric warmings or have no stratospheric response 15 to 45 days after
179 they were observed. These instances represent roughly half of the positive SLP anomalies
180 of similar magnitude, which are at least one standard deviation above the area-averaged
181 climatology.

182 Next, we repeat the analysis in Figure 1 for geopotential heights at 200 hPa in order to
183 compare anomalies in the upper troposphere to the lower troposphere. Polvani and Waugh
184 (2004) argue that upward propagating WAF near the tropopause is important to
185 stratospheric variability. Following stratospheric warming events (Figures 2b and 2d),
186 height anomalies are positive over the Arctic consistent with a barotropic structure of the
187 tropospheric response following stratospheric warmings. Prior to stratospheric warmings
188 (Figures 2a, c) the tropospheric structure is more baroclinic with negative height anomalies
189 at 200 hPa above the positive height anomalies in the lower troposphere. The Siberian high
190 is a shallow feature extending from the surface to as high as 500 hPa. Increased troughing
191 and anomalously low heights over Siberia is consistent with cooling of the atmospheric
192 column due to snow cover and stronger high pressure at the surface. Comparing Figures 1
193 and 2, we note that differences are greater in the lower troposphere than in the upper
194 troposphere prior to vortex displacements and splits.

195

b. Wave activity flux and polar-cap geopotential height anomalies

We next present in Figure 3 the 15-day mean anomalies in the three-dimensional wave energy flux that vertically propagates from Rossby waves prior to both vortex displacements and splits at 100 hPa. The six-week absorption of positive anomalous WAF in the stratosphere has been shown to precipitate stratospheric warmings (Polvani and Waugh 2004). Furthermore Smith et al. (2011) show that planetary–scale waves (waves one and two) contribute most to the variability in WAF while synoptic-scale waves contribute relatively much less to the variability in WAF. Given that the anomalous height field forms either a wave one or a wave two pattern prior to vortex displacements and splits respectively, we would expect that the tropospheric precursors presented in Figure 1, to have a strong influence on the variability in the vertical WAF.

Prior to vortex displacements, there is a slow build-up in the upward WAF starting six weeks prior to the stratospheric warming event, which peaks the last two weeks prior to the stratospheric warming event. The upward WAF anomalies are centered over Eurasia, in particular Siberia, and extend out into the North Pacific. Similarly, prior to vortex splitting events there is also a slow build-up in upward WAF six weeks prior to the splitting event that peaks the last two weeks prior to the stratospheric warming. There is a strong focus of anomalies over Siberia, however, in contrast to the vortex displacements, the peak upward WAF anomaly is absent from western Eurasia and instead there exist additional anomaly centers over North America and the North Atlantic sector.

Next, we present the area-weighted polar cap geopotential height anomalies and WAF anomalies over the Eurasian sector for vortex displacements in Figure 4a and splits in Figure 4c throughout the atmospheric column. Also shown is the statistical significance of both

variables for displacements (Figure 4b) and splits (Figure 4d). Prior to vortex displacements there are two preceding events seen in the plot. First, is a positive height anomaly averaged around the polar cap in the troposphere thirty days and even as early as six weeks prior to the stratospheric warming and peaks two to three weeks prior to the stratospheric warming event. This positive polar cap anomaly is a result of the strengthened Siberian high and the increased heights northwest of the climatological center as seen in Figure 1. Polar cap heights are positive in the troposphere despite the deepened Aleutian low and lower heights in that region. The second event is the upward pulse of WAF that builds in the lower troposphere and eventually breaks through into the stratosphere where it peaks just days before the climax in the stratospheric warming event. What is also noted from the plot is that the upward WAF pulse strengthens as the tropospheric precursor weakens; see further discussion below. Following the stratospheric warming event, the upward WAF ceases and instead the downward propagation of the high heights is seen during the following six weeks and culminates in an annular mode pattern in the troposphere as seen in Figure 1 and as shown previously (Baldwin and Dunkerton 1999; Baldwin et al. 2003).

Prior to vortex splits, there is not evident in the polar cap diagnostic a long-lead coherent tropospheric precursor as seen for vortex displacements. There is some suggestion of a tropospheric precursor a week before the stratospheric warming event, but earlier the heights are mostly of the opposite sign. However, post the stratospheric warming event, the downward propagation of positive height anomalies is observed, culminating with the annular mode pattern in the lower troposphere similar to vortex displacement events.

Next, in Figure 5, we present the time series of the SLP anomalies in the region of the strengthened Siberian high in northern Eurasia and the upward WAF anomalies at 100hPa in the Eurasian sector for vortex displacements. The highest positive SLP anomalies are

242 associated with the tropospheric precursor 15 to 30 days prior to the stratospheric warming
243 event. Simultaneously, there is a relative minima in the upward WAF flux or a relaxation to
244 climatological values, which is consistent with the building of lower tropospheric heights.
245 Then, starting three weeks prior to the warming, SLP anomalies fall precipitously while
246 simultaneously the upward WAF turns strongly positive and peaks just prior to the
247 stratospheric warming and then returns to normal levels post the stratospheric warming.
248 Also post the stratospheric warming, SLP anomalies slowly build, reaching a secondary
249 maximum over a month after the stratospheric warming and a season or 90 days after the
250 development of the tropospheric precursor. On the bottom axis we have included the
251 average date to provide an approximate or mean timing of these events. We argue that not
252 only does this plot demonstrate the potential application of this analysis for improved
253 seasonal prediction, with an increased lead time of at least thirty days compared with using
254 the stratosphere, but provides a tangible target for modelers for improved simulation of
255 winter climate. The inability of dynamical climate models to simulate important physical
256 processes contributes to forecast error on seasonal time scales (Doblas-Reyes et al. 2009).

257 A similar plot for the SLP time series for vortex splits does not show the same features as
258 was seen for vortex displacements (Panel 5b). There is a building of high pressure over a
259 month earlier than the stratospheric warming event, but it is not statistically significant.
260 However, the strong upward WAF is seen just prior to the stratospheric warming as in the
261 displacement events, though there are two separate large pulses in contrast to the one large
262 pulse observed prior to vortex displacements.

263 *c. Differences between precursors to displacements and splits*

We performed further analysis to distinguish whether the differences seen in the tropospheric precursor in Figures 1 and 5 are significant. We computed a tripole index where we took the difference in the area-averaged SLP in the region of the Siberian high, the Aleutian low and the midlatitudes of the North Atlantic between vortex displacements and splits starting from 45 days before until 45 days after the stratospheric warming events, shown in Figure 5c. The time series shows that the largest, as well as statistically significant, differences between the two time series occur between four and two weeks before the stratospheric warming. This is the critical period when the main pulses of WAF are initiated for both vortex displacements and splits. We further tested the significance of the difference in the SLP field associated with displacements and splits by taking random samples from the observed data and computed the same tripole index as shown in Figure 5c. We found that the likelihood of SLP differences of similar magnitude to the composite of differences prior to splits and displacements to be less than 1% simply due to chance.

In Figure 6, we present SLP anomalies from 28 to 7 days averaged every 7 days prior to vortex displacements and splits. Prior to vortex displacements there are two dominant centers of SLP anomalies one associated with the Siberian high and the other with the Aleutian low; together they form a clear wave-one pattern across the mid to high latitudes. Prior to vortex splits, the SLP anomalies are more diffuse and do not form a clear dipole, but instead may be better described as a shift in the storm tracks in the respective ocean basins. And though there is a positive SLP anomaly centered near northwest Eurasia, at least initially it does not seem to be associated with the Siberian high. However, closer in time to the stratospheric warming event this positive SLP anomaly propagates eastward and is absorbed into the Siberian high. In contrast prior to vortex displacements, the dominant positive SLP anomaly propagates westward away from the Siberian high closer in time to the stratospheric warming. It is accepted that Arctic outbreaks across Europe are associated

289 with the Siberian high, but this is the first time that we are aware of the westward
290 propagation of Arctic high pressure associated with the Siberian high has been demonstrated
291 for Europe. This is an active area of ongoing research.

292 Finally, we also analyzed the weekly accumulative snow cover extent anomalies for Eurasia.
293 Snow cover extent is measured as a frequency of time when snow cover is observed over a
294 given grid box. Prior to and during the building of the strong high pressure and increased
295 upward WAF, there is a rapid increase in snow cover in the region of the development of the
296 high pressure prior to vortex displacements (Figure 7a). The increase in snow cover extent
297 across the Northern Hemisphere (only Eurasia is shown) is greatest close to the positive SLP
298 anomaly center that is associated with the northwestward expansion of the Siberian high as
299 shown in Figures 1a and 6a. Prior to vortex splits, there is also a rapid increase in snow
300 cover anomalies prior to the building of high pressure and increased upward WAF as seen
301 with displacements (Figure 7b). However, the increase in snow cover is focused closer to
302 Scandinavia just as the positive SLP anomaly prior to vortex splits is focused closer to
303 Scandinavia as seen in Figure 6d.

304 **4. Conclusions**

305 Until recently, vortex displacements and splits have been mostly grouped together probably
306 because, as shown by Charlton and Polvani (2007) and as we show here, following both
307 events the tropospheric response most closely resembles a negative annular mode pattern for
308 both events. However, prior to both events the tropospheric forcing and the upward
309 propagation of energy emanating from the large tropospheric waves display similarities, but
310 also important differences in the presented analysis. A distinct tropospheric precursor is
311 identified thirty days or even six weeks prior to the stratospheric vortex displacement event.
312 The precursor to a vortex displacement involves two of the three main centers of action in

313 the Northern Hemisphere, with a strengthened Siberian high and a deepened Aleutian low.
314 In contrast for vortex splits, the tropospheric precursor resembles a meridional shift in the
315 major storm tracks, more so than a strengthened center of action. A second important
316 distinction is in the upward anomalies of wave-driven energy. The upward pulse in WAF
317 has origins in the lower troposphere prior to the main upward pulse. However from our
318 analysis this is more clearly seen for vortex displacements than vortex splits and therefore
319 vortex displacements are more easily associated with boundary forcings such as snow cover
320 and possibly even ENSO when compared with vortex splits. And as seen in Figure 5, the
321 SLP field and the WAF have a unique signature beginning over a month prior to the
322 stratospheric warming and a full season prior to the peak in the surface annular mode event.
323 This signature in the respective fields can be exploited for improved simulations of modeled
324 winter climate and seasonal predictions. Currently, numerical models have been shown to
325 be deficient in predicting atmospheric blocking events (Tracton et al. 1989) and are deficient
326 in simulating troposphere-stratosphere coupling (Hardiman et al. 2008). Identification of
327 precursors may not only advance seasonal forecasting beyond its dependence on ENSO
328 (Cohen and Fletcher 2007), but may also help modelers improve global climate model
329 simulations of present and future winter climate.

330

331 **Acknowledgements**

332 JC is supported by the National Science Foundation grants ARC-0909459 and ARC-
333 0909457 and NOAA grant NA10OAR4310163.
334

335 **References**

336 Allen, R. J., and C. S. Zender, 2010: Effects of continental-scale snow albedo anomalies on
337 the wintertime Arctic oscillation. *J. Geophys. Res.*, **115**, D23105,
338 doi:10.1029/2010JD014490.
339 Baldwin, M. P., and T. J. Dunkerton, 1999: Propagation of the Arctic Oscillation from the
340 stratosphere to the troposphere. *J. Geophys. Res*., **104**, 30,937-30,946.
341 Baldwin, M. P., and T. J. Dunkerton, 2001: Stratospheric harbingers of anomalous weather
342 regimes. *Science,* **294**, 581-584.
343 Baldwin, M. P., D. B. Stephenson, D. W. J. Thompson, T. J. Dunkerton, A. J. Charlton, and
344 A. O'Neill, 2003: Stratospheric memory and extended-range weather forecasts.
345 *Science,* **301**, 636-640.
346 Charlton A. J., and L. M. Polvani, 2007: A new look at stratospheric sudden warmings.
347 Part I. Climatology and modeling benchmarks. *J. Climate,* **20**, 449-469.
348 Charlton A. J., A. O'Neill, D. B. Stephenson, W. A. Lahoz, and M. P. Baldwin, 2003: Can
349 knowledge of the state of the stratosphere be used to improve statistical forecasts of
350 the troposphere? *QJRMS,* **129**, 3202-3225.
351 Charney, J. G. and P. G. Drazin, 1961: Propagation of planetary-scale disturbances from
352 the lower into the upper atmosphere. *J. Geophys. Res*., **66**, 83-109.
353 Cohen, J., 2003: Introducing sub-seasonal and temporal resolution to winter climate
354 prediction. *Geophys. Res. Lett*. **30**, 1018, doi:10.1029/2002GL016066.
355 Cohen, J., and D. Entekhabi, 1999: Eurasian snow cover variability and Northern
356 Hemisphere climate predictability. *Geophys. Res. Lett*., **26**, 345-348.

357 Cohen, J., and C. Fletcher, 2007: Improved Skill for Northern Hemisphere winter surface
358 temperature predictions based on land-atmosphere fall anomalies. *J. Climate,* **20**,
359 4118-4132.
360 Cohen, J., K. Saito, and D. Entekhabi, 2001: The role of the Siberian high in Northern
361 Hemisphere climate variability. *Geophys. Res. Lett*., **28**, 299-302.
362 Cohen, J., D. Salstein, and K. Saito, 2002: A dynamical framework to understand and
363 predict the major Northern Hemisphere mode. *Geophys. Res. Lett*., **29**, 1412.
364 Cohen, J., M. Barlow, P. Kushner, and K. Saito, 2007: Stratosphere-Troposphere coupling
365 and links with Eurasian Land-Surface Variability. *J. Climate,* **20**, 5335–5343.
366 Doblas-Reyes, F. J. and co-authors, 2009: Addressing model uncertainty in seasonal and
367 annual dynamical ensemble forecasts. *QJRMS,* **135**, 1538-1559.
368 Feldstein, S. B. and C. Franzke, 2006: Are the North Atlantic Oscillation and the Northern
369 Annular Mode Distinguishable? *J. Atmos. Sci.,* **64**, 2915–2930.
370 Garfinkel, C. I., D. L. Hartmann, and F. Sassi, 2010: Tropospheric Precursors of
371 Anomalous Northern Hemisphere Stratospheric Polar Vortices. *J. Climate,* **23**,
372 3282-3299.
373 Hardiman, S. C., P. J. Kushner, and J. Cohen, 2008: Investigating the ability of general
374 circulation models to capture the effects of Eurasian snow cover on winter climate.
375 *J. Geophys. Res.,* **113**, D21123.
376 Ineson, S., and A. A. Scaife, 2009: The role of the stratosphere in the European climate
377 response to El Niño. *Nature Geosci*., **2**, 32-36.

Kalnay, E. et al., 1996: The NCEP/NCAR 40-Year reanalysis project. *Bull. Amer. Meteor. Soc.,* **77**, 437-471.

Kolstad, E. W., and A. J. Charlton-Perez, 2010: Observed and simulated precursors of stratospheric polar vortex anomalies in the Northern Hemisphere. *Climate Dynamics,* in press.

Manney, G. L., K. Kruger, J. L. Sabutis, S. A. Sena, and S. Pawson, 2005: The remarkable 2003–2004 winter and other recent warm winters in the Arctic stratosphere since the *late 1990s.* J. Geophys. Res*., 110, D04107.*

Martius, O., L. M. Polvani, and H. C. Davies, 2009: Blocking pre- cursors to stratospheric sudden warming events. *Geophys. Res. Lett.,* **36**, L14806.

Matsuno, T., 1970: Vertical propagation of stationary planetary waves in the winter Northern Hemisphere. *J. Atmos. Sci*., **27**, 871-883.

Orsolini Y. J. and N. G. Kvamsto, 2009: Role of Eurasian snow cover in wintertime circulation: Decadal simulations forced with satellite observations. *J. Geophys. Res.,* **114**, D19108.

Plumb, R. A., 1985: On the three-dimensional propagation of stationary waves. *J. Atmos. Sci.,* **42**, 217-229.

Plumb, R. A., and K. Semeniuk, 2003: Downward migration of extratropical zonal wind anomalies. *J. Geophys. Res*., **108**, 4223.

Polvani, L. M., and D. W. Waugh, 2004: Upward Wave Activity Flux as Precursor to Extreme Stratospheric Events and Subsequent Anomalous Surface Weather Regimes. *J. Climate,* **17**, 3548-3554.

400 Scinocca, J. F., and P. H. Haynes, 1998: Dynamical forcing of stratospheric waves by the
401 tropospheric circulation. *J. Atmos. Sci*, **55,** 2361–2392.
402 Seager, R., Y. Kushnir, J. Nakamura, M. Ting, and N. Naik, 2010: Northern Hemisphere
403 winter snow anomalies: ENSO, NAO and the winter of 2009/10. *Geophys. Res.*
404 *Lett*. **37**, L1470.
405 Smith, K. L., C. G. Fletcher, and P. J. Kushner, 2010: The role of linear interference in the
406 Annular Mode response to extratropical surface forcing. *J. Climate,* **23**, 6036-6050.
407 Smith, K., P. J. Kushner and J. Cohen, 2011: The role of linear interference in Northern
408 Annular Mode variability associated with Eurasian snow cover extent, *J. Climate*, in
409 review.
410 Ting, M. F. and I. M. Held, 1990: The Stationary Wave Response to a Tropical SST
411 Anomaly in an Idealized GCM. *J. Atmos. Sci.*, **47**(21): 2546-2566.
412 Tracton, M. S., and coauthors, 1989: Dynamical extended range forecasting (DERF) at the
413 National Meteorological Center. *Mon. Wea. Rev*. **117**, 1604-1635.
414 Uppala et al., 2006: The ERA-40 re-analysis. *QJRMS,* **131**, 2961-3012.

415

416
417

417 **Table Legends**

418 Table 1. Central date for vortex displacements and vortex splits.

419

Figure Legends

Figure 1. Sea level pressure anomalies a) averaged 45 to 0 days prior to vortex displacements b) averaged 0 to 45 days after vortex displacements c) averaged 45 to 0 days prior to vortex splits d) averaged 0 to 45 days after vortex splits. Colored shading represents anomalies in hPa, solid contours show the full values of the sea level pressure field and dashed contours represent 90 and 95% confidence levels. Mean values are computed daily over the reanalysis time period 1948-2010.

Figure 2. Same as Figure 1 but for 200 hPa and in decameters.

Figure 3. Vertical wave activity flux (WAF) anomalies at 100 hPa a) averaged 45 to 30 days prior to vortex displacements b) averaged 30 to 15 days prior to vortex displacements c) averaged 15 to 0 days prior to vortex displacements d) averaged 45 to 30 days prior to vortex splits e) averaged 30 to 15 days prior to vortex splits f) averaged 15 to 0 days prior to vortex splits. WAF anomalies shaded in m^2s^{-2}.

Figure 4. Polar cap geopotential height anomalies (shading) and wave activity flux anomalies bounded by 40-80°N and 30-180°E (contouring) from 45 days prior until 45 days after a) vortex displacements and b) vortex splits. Values shaded and contoured every 0.2 standardized anomalies. Also shown are only those values for geopotential height anomalies (shown in solid contours) found to be statistically significant at the 95% confidence level or higher (blue shading) and those WAF values (shown in dashed contouring) found to be statistically significant at the 95% confidence level or higher (red shading) for b) vortex displacements and d) vortex splits.

442 **Figure 5.** Area averaged daily sea level pressure anomalies in the area bounded by 60-75°N
443 and 30-90°E (black line) and wave activity flux anomalies over the Eurasian sector (blue
444 line) for a) vortex displacements and b) vortex splits. c) The sum of the area averaged
445 difference in SLP for the boxes bounded by 55-70°N and 30-90°E, 55-70°N and 120-
446 180°W, 40-50°N and 30-60°W for vortex displacements and splits. Red and green symbols
447 represent 95% significance for SLP and WAF anomalies respectively. SLP anomalies
448 given in hPa and WAF anomalies in m^2s^{-2} multiplied by 25. Top axis of a), b) and c) and
449 bottom axis of c) represent days before and after stratospheric warming event and bottom
450 axis in a) and b) shows mean calendar date.

451 **Figure 6.** Sea level pressure anomalies a) averaged 28 to 21 days prior to vortex
452 displacements b) averaged 21 to 14 days prior to vortex displacements c) averaged 14 to 7
453 days prior to vortex displacements d) averaged 28 to 21 days prior to vortex splits e)
454 averaged 21 to 14 days prior to vortex splits f) averaged 14 to 7 days prior to vortex splits.
455 Colored shading represents anomalies in hPa, solid contours show the full values of the sea
456 level pressure field. Mean values are computed daily over the reanalysis time period 1948-
457 2010.

458

459 **Figure 7.** a) Change in snow cover extent two to four weeks prior to a vortex displacement
460 across Eurasia and b) change in snow cover extent two to four weeks prior to a vortex split
461 across Eurasia.

462

463

463

Vortex Displacements – Central Date		Vortex Splits – Central Date	
30	November 1958	30	January 1958
16	January 1960	23	March 1965
08	December 1965	24	February 1966
27	November 1968	08	January 1968
13	March 1969	17	January 1971
02	January 1970	02	February 1973
20	March 1971	22	February 1979
29	February 1980	02	January 1985
04	December 1981	08	December 1987
24	February 1984	14	March 1988
23	January 1987	22	February 1989
15	December 1998	25	February 1999
20	March 2000	11	February 2001
16	December 2000	18	January 2003
02	January 2002	21	January 2006
07	January 2004	24	January 2009
24	February 2007	09	February 2010
22	February 2008		

464

465 **Table 1.** Central date for vortex displacements and vortex splits.

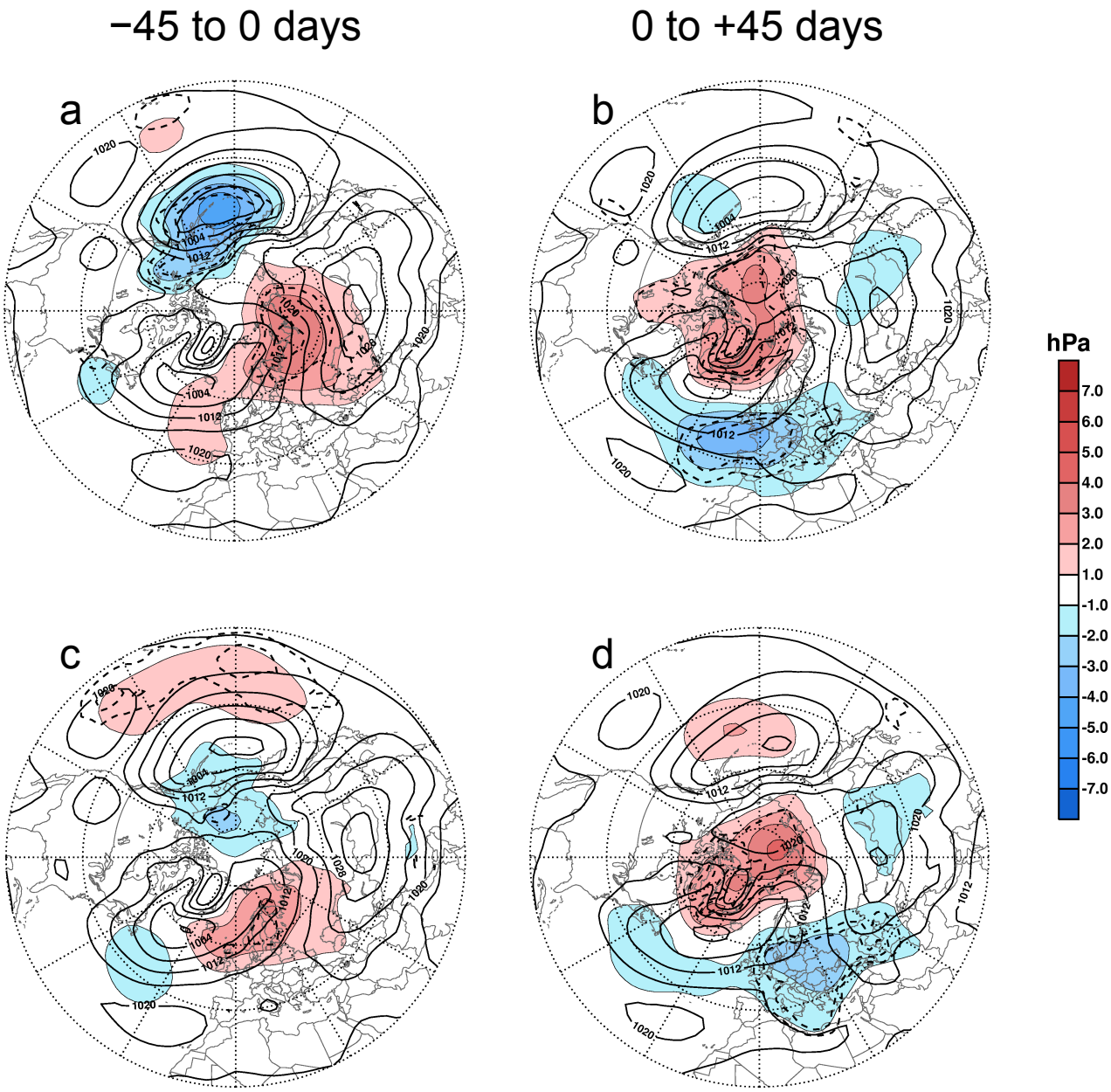

Figure 1. Sea level pressure anomalies a) averaged 45 to 0 days prior to vortex displacements b) averaged 0 to 45 days after vortex displacements c) averaged 45 to 0 days prior to vortex splits d) averaged 0 to 45 days after vortex splits. Colored shading represents anomalies in hPa, solid contours show the full values of the sea level pressure field and dashed contours represent 90 and 95% confidence levels. Mean values are computed daily over the reanalysis time period 1948-2010.

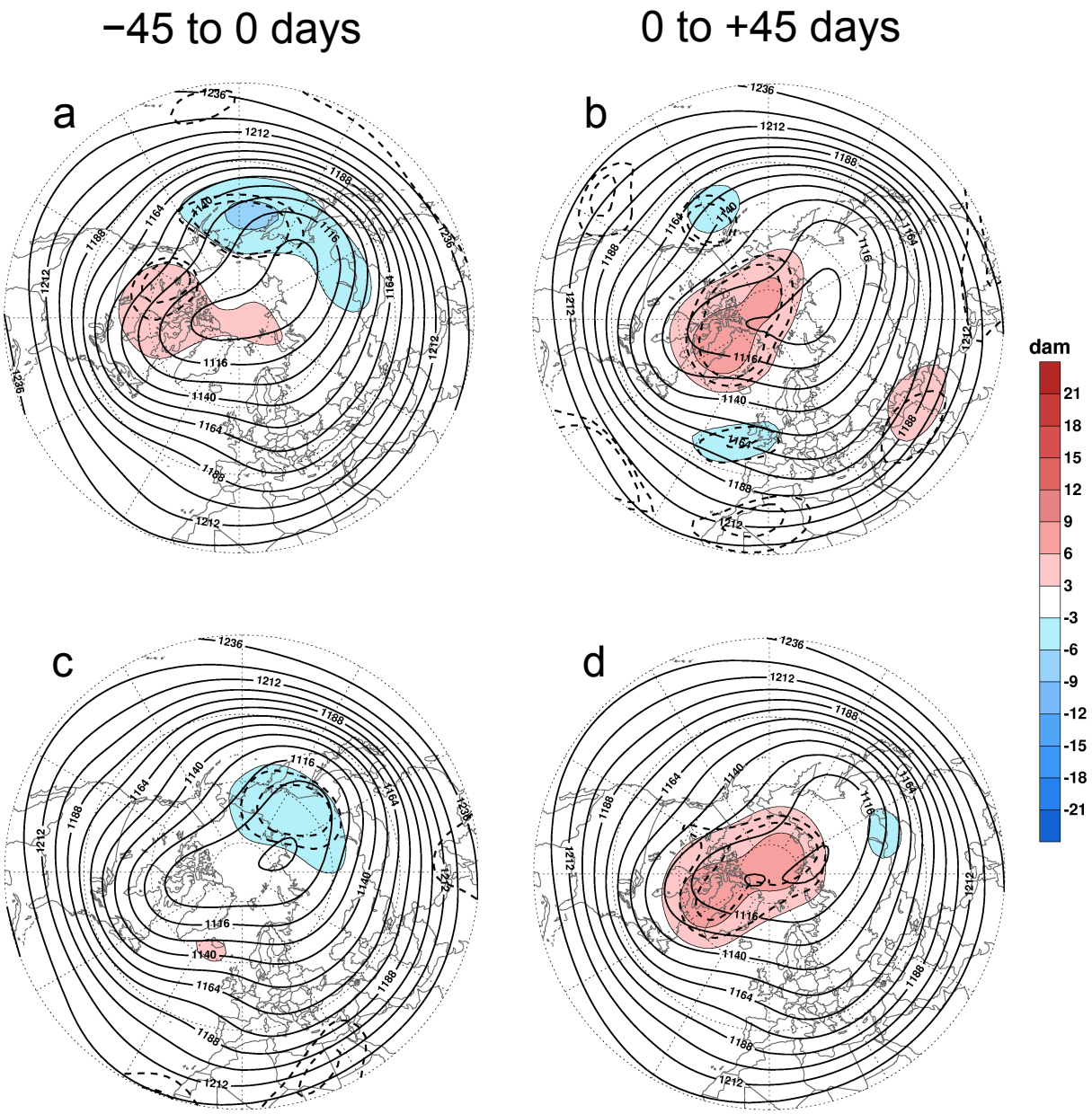

Figure 2. Same as Figure 1 but for 200 hPa and in decameters.

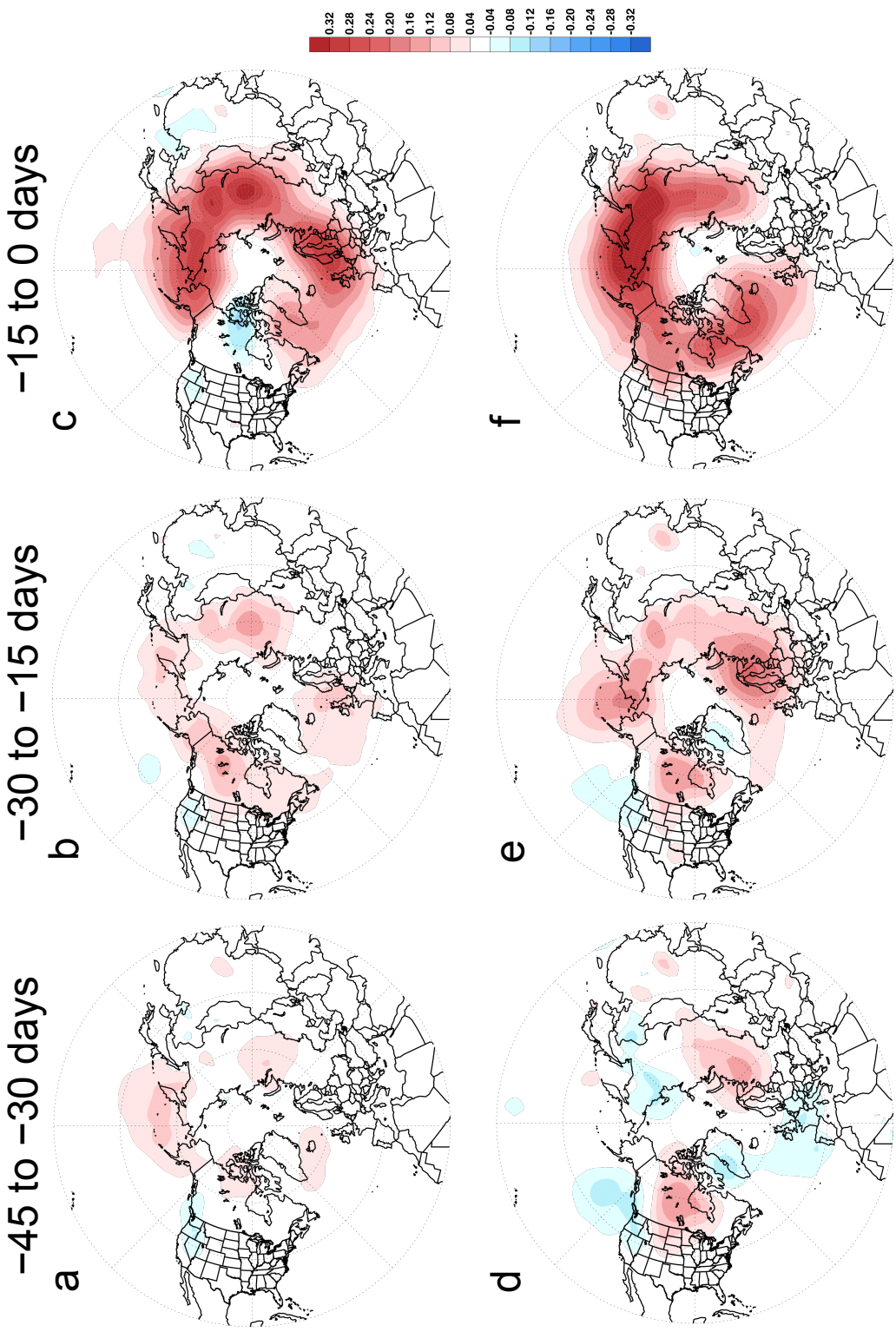

Figure 3. Vertical wave activity flux (WAF) anomalies at 100 hPa a) averaged 45 to 30 days prior to vortex displacements b) averaged 30 to 15 days prior to vortex displacements c) averaged 15 to 0 days prior to vortex displacements d) averaged 45 to 30 days prior to vortex splits e) averaged 30 to 15 days prior to vortex splits f) averaged 15 to 0 days prior to vortex splits. WAF anomalies shaded in m^2s^{-2}.

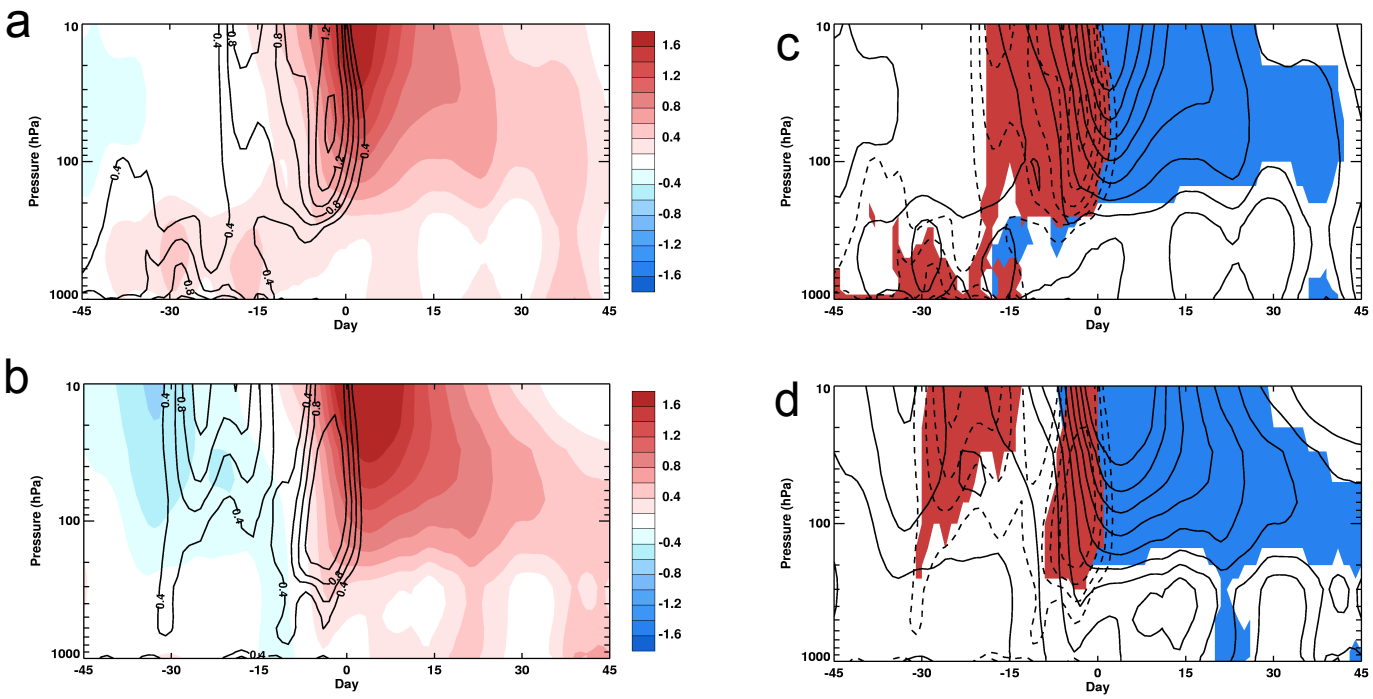

Figure 4. Polar cap geopotential height anomalies (shading) and wave activity flux anomalies bounded by 40-80°N and 30-180°E (contouring) from 45 days prior until 45 days after a) vortex displacements and b) vortex splits. Values shaded and contoured every 0.2 standardized anomalies. Also shown are only those values for geopotential height anomalies (shown in solid contours) found to be statistically significant at the 95% confidence level or higher (blue shading) and those WAF values (shown in dashed contouring) found to be statistically significant at the 95% confidence level or higher (red shading) for b) vortex displacements and d) vortex splits.

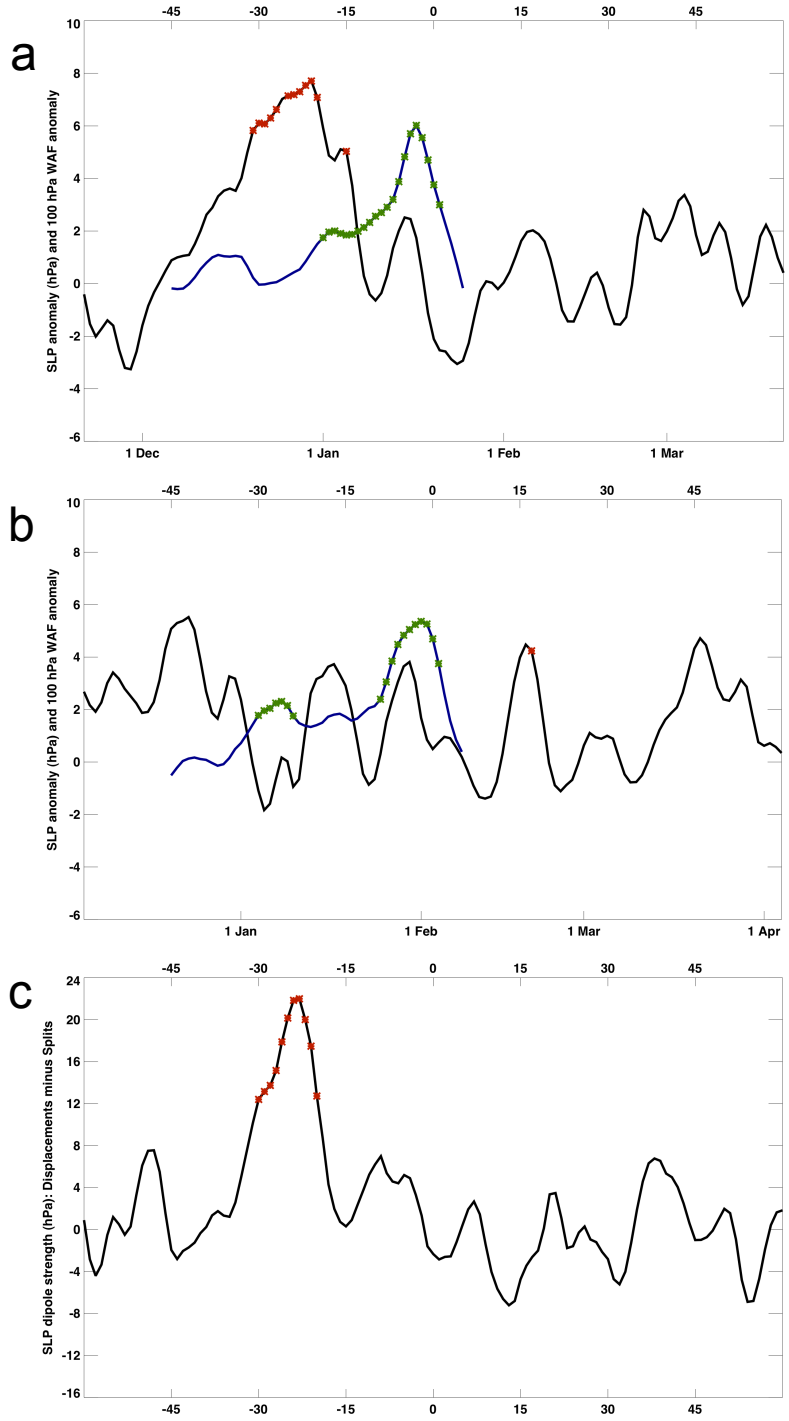

Figure 5. Area averaged daily sea level pressure anomalies in the area bounded by 60-75°N and 30-90°E (black line) and wave activity flux anomalies over the Eurasian sector (blue line) for a) vortex displacements and b) vortex splits. c) The sum of the area averaged difference in SLP for the boxes bounded by 55-70°N and 30-90°E, 55-70°N and 120-180°W, 40-50°N and 30-60°W for vortex displacements and splits. Red and green symbols represent 95% significance for SLP and WAF anomalies respectively. SLP anomalies given in hPa and WAF anomalies in m^2s^{-2} multiplied by 25. Top axis of a), b) and c) and bottom axis of c) represent days before and after stratospheric warming event and bottom axis in a) and b) shows mean calendar date.

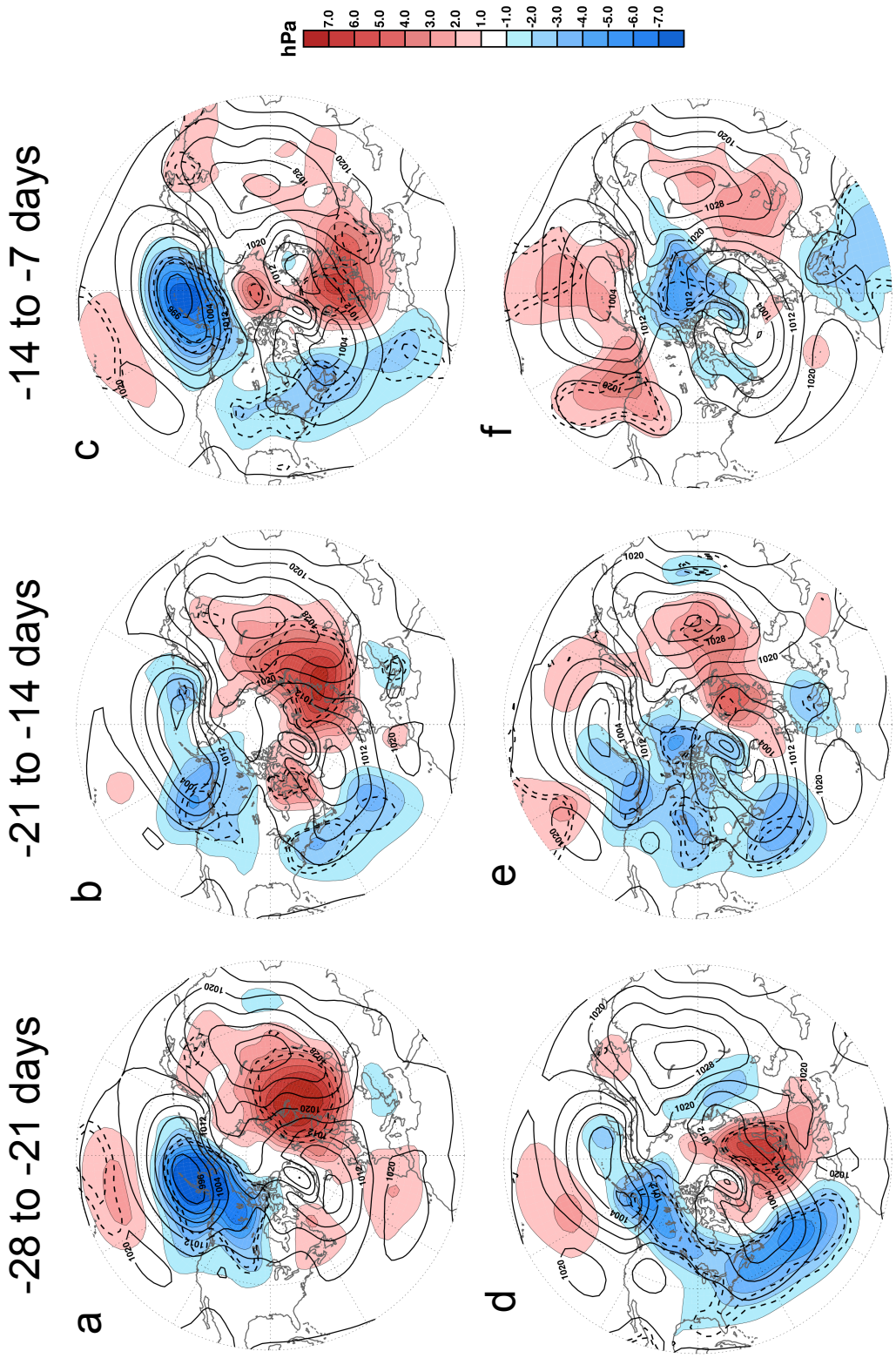

Figure 6. Sea level pressure anomalies a) averaged 28 to 21 days prior to vortex displacements b) averaged 21 to 14 days prior to vortex displacements c) averaged 14 to 7 days prior to vortex displacements d) averaged 28 to 21 days prior to vortex splits e) averaged 21 to 14 days prior to vortex splits f) averaged 14 to 7 days prior to vortex splits. Colored shading represents anomalies in hPa, solid contours show the full values of the sea level pressure field. Mean values are computed daily over the reanalysis time period 1948-2010.

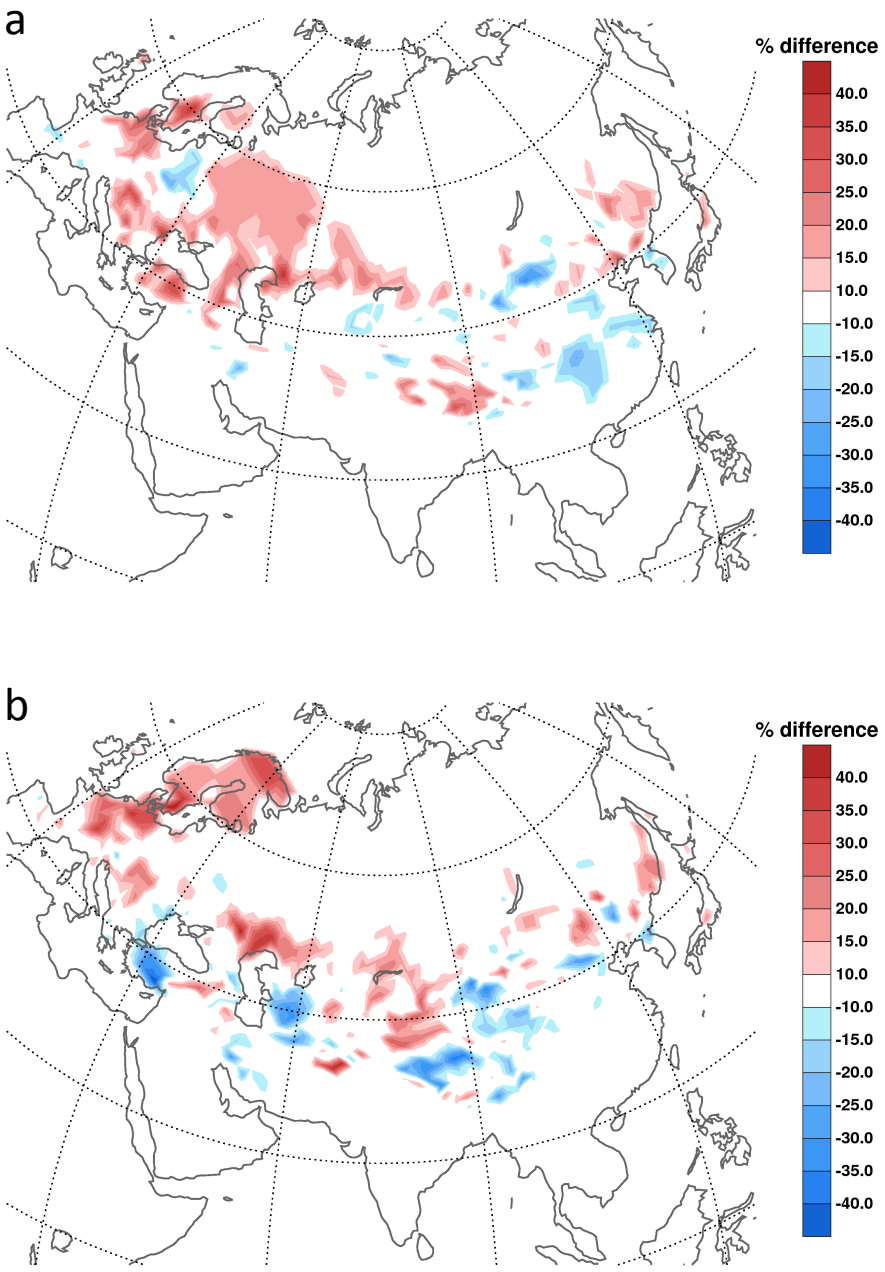

Figure 7. a) Change in snow cover extent two to four weeks prior to a vortex displacement across Eurasia and b) change in snow cover extent two to four weeks prior to a vortex split across Eurasia.